Acta Ophthalmologica

Elevated intraocular pressure induces neuron-specific β-III-tubulin expression in non-neuronal vascular cells

Verena Prokosch,[1,2,†] Kathrin Brockhaus,[1,†] Fabian Anders,[2] Hanhan Liu,[2] Karl Mercieca,[3] Adrian Gericke,[2] Harut Melkonyan[1] and Solon Thanos[1]

[1]Institute of Experimental Ophthalmology and DFG-Center of Excellence, Cells in Motion (CIM), School of Medicine, Westfalian-Wilhelms-University of Münster, Munster, Germany
[2]University Eye Hospital Mainz, Johannes Gutenberg University of Mainz, Mainz, Germany
[3]Manchester Royal Eye Hospital, Manchester, UK

ABSTRACT.

Purpose: **Pathological alterations within optic nerve axons and progressive loss of the parental retinal ganglion cell (RGC) bodies are characteristics of glaucomatous neuropathy. Abnormally elevated intraocular pressure (IOP) is thought to be the major risk factor for most forms of glaucomatous changes, while lowering of the IOP is the mainstream of treatment. However, the pathophysiological mechanisms involved in neurodegenerative changes are poorly understood. It remains still a matter of debate whether elevated IOP harms the neurons directly or indirectly through alterations in the retinal vascularization.**

Methods: **We analysed morphological and molecular changes within the retina exposed to elevated IOP in an animal model of glaucoma *in vivo*, in retinal explants and in cultured dissociated retinal cells each incubated under elevated air pressure *in vitro*, imitating elevated IOP.**

Results: **Although ß-III-tubulin expressing RGCs decreased within the course of the disease, total amount of ß-III-tubulin protein within the retina increased, leading to the assumption that other cells than RGCs abnormally express ß-III-tubulin due to elevated IOP. Surprisingly, we found that β-III-tubulin, a marker developmentally regulated and specifically expressed in neurons under normal conditions, was strongly up-regulated in desmin-, PDGFR-β- and α-SMA-positive pericytes as well as in endothelin-1-positive endothelial cells both *in vivo* under elevated IOP and *in vitro* under elevated culture atmosphere pressure that simulated IOP elevation. Beta-III-tubulin-driven signalling pathways (ERK 1/2, pERK1/2 and cdc42/Rac) were also regulated.**

Conclusion: **The unprecedented regulation of neuron-specific β-III-tubulin in pericytes and endothelial cells is likely associated with a role of the retinal vasculature in the IOP-induced development and manifestation of glaucomatous degenerative optic nerve response.**

Key words: cell cultures – glaucoma – retinal biomarkers – vascular endothelial cells – vascular pericytes – β-III-tubulin

[†]Shared first author.

Acta Ophthalmol. 2020: 98: e617–e630

doi: 10.1111/aos.14333

Introduction

Retinal and optic neuropathy due to abnormal elevation of intraocular pressure (IOP) is one of the leading causes of blindness (Quigley & Broman 2006). Structurally, glaucomatous neuropathy is characterized by progressive degeneration of optic nerve axons and the retrograde death of retinal ganglion cells (RGCs) resulting in ophthalmoscopically visible atrophy of the optic nerve head and functionally in progressive narrowing of the visual field. Interestingly, although elevated IOP is identified as a primary risk factor for development of glaucomatous neuropathy, the disease may progress

despite normalization of the IOP (Leske 2007) indicating that once initiated, molecular events may go on independent of the IOP-level. The pathophysiological mechanisms involved in glaucomatous changes are poorly understood. Self-operating signalling may be localized within the retina, choroidal or peripapillary structures (Kornzweig et al. 1968; Grunwald et al. 1984; Ullrich et al. 1996). It remains still unclear whether elevated IOP harms the neurons directly or whether elevated IOP may first provoke alterations, for example, in vascular cells which harm the neurons indirectly in a second step. Increasing attention is being paid to the role of alterations in vascular blood supply in the context of glaucoma.

One of the mechanisms maintaining regressive changes even after IOP normalization may be driven by decreased blood flow in the optic nerve head, retina and choroid (Kornzweig et al. 1968; Riva et al. 1981; Grunwald et al. 1984; Michelson et al. 1996; Grunwald et al. 1998; Findl et al. 2000; Wang 2011). The molecular mediators between glaucomatous neuropathy and blood flow capacity seem to be associated with the endothelial system (Eisner et al. 1995; Kaiser 1995; Sugiyama et al. 1995; Chauhan et al. 2002; Flammer & Mozaffarieh 2008; Resch et al. 2010; Galassi et al. 2011). Dysregulation of ocular circulation may be combined with activation of retinal glial cells building the ground for pathogenetic events during onset and establishment of glaucoma (Prasanna et al. 2011).

An increasing number of studies have shown that the dynamic regulation of microtubules in moving cells plays an essential role in cell steering. Class β-III-tubulin is a constituent of neuronal microtubules and is frequently used as a marker of RGCs within the retina (Sharma & Netland 2007). The marker is not solely expressed by RGCs and is rather related to the cell lineage during neurogenesis (Sharma & Netland 2007). In accordance, class β-III-tubulin is expressed in retinal neurons within the human retina, whereas it is aberrantly expressed in cultured retinal pigment epithelial cells with differentiated morphologies (Vinores et al. 1995). In the normal adult retina and CNS, the distribution of class β-III-tubulin is almost exclusively neuron specific, while altered expression is observed in brain tumours such as medulloblastomas. During neurogenesis, β-III-tubulin is neuron associated and shows certain temporospatial gradients during cerebellum and telencephalic development with transient expression in putative neuronal and glial cells (Vinores et al. 1995). In peripheral perivascular cells, β-III-tubulin is expressed during remodelling of adult rat mesenteric network (Stapor & Murfee 2012). In the CNS and PNS, β-III-tubulin is expressed in glial and neural progenitor cells (Katsetos et al. 2003; Draberova et al. 2008). β-III-tubulin is expressed neither in adult glial nor in vascular cells.

The development of effective treatment of glaucomatous neuropathy requires a fundamental understanding of the cellular responses to elevation of IOP. This includes the responses of capillary endothelial cells and pericytes, together with all glial and neuronal retinal and optic nerve elements (Ozerdem & Freeman 2001; Peirce & Skalak 2003; Murfee et al. 2005).

In the present work, we induced elevated IOP in rats and examined expression of β-III-tubulin within the retina in the course of the disease. We will show for the first time that β-III-tubulin is not solely expressed in RGCs, but abundantly in capillary endothelial cells and vascular pericytes, hinting at the fact that IOP may alter the vascular network directly.

Methods

Animals and drugs

All experiments were conducted in accordance with the Association for Research in Vision and Ophthalmology Statement on the Use of Animals in Ophthalmic and Vision Research. Female Sprague Dawley rats weighing 108–250 g were housed in a standard animal room under a 12-hr light/dark cycle with food and water provided ad libitum. The ethics committee (regional government of Münster) approved this study (permission Nr.: 84-02.04.2011.A132). Surgical procedures were performed unilaterally, on the left eye under general anaesthesia induced by a mixture of 2 mg/kg body weight ketamine and 2 mg/kg body weight xylazine (Leva-Sanofi, Düsseldorf, Germany), administered intraperitoneally. After each surgical intervention, antibiotic eye ointment (Gentamytrex, Dr. Mann Pharma, Berlin, Ge) was applied locally. The animal health and behaviour were monitored postoperatively at regular intervals. The experimental follow-up after cauterization lasted 8 weeks. Each experimental group comprised 13 animals, except for the iridectomy group comprising five animals.

Induction of glaucoma and IOP measurement

Intraocular pressure was elevated through thermic cauterization of three episcleral veins as described previously (Prokosch et al. 2013). Briefly, the limbus-draining veins travelling close to the sclera and anastomosing at the equator of the eye were exposed by incision of the conjunctiva where they build four to five major venous trunks almost equidistant around the circumference of the globe. Ophthalmic cautery was applied to three of these large veins per eye, resulting in blockage of more than 50% of the venous outflow. Care was taken not to perforate the sclera during this procedure. An uncauterized group ($n = 13$) served as the normotensive control. One group of animals ($n = 13$) remained with a persistent elevated IOP. Hypotension treatment was performed surgically by iridectomy ($n = 5$). For this, a small paracentesis was done at the corneal limbus at 1 o'clock. Protruded iris was cut with the iridectomy scissor, and the remaining iris was reposited into the anterior chamber. Intraocular pressure (IOP) measurements were made before and immediately after cauterization and then every week between 9.00 a.m. and 12.00 a.m. with topically applied 0.5% proparacaine (URSA-Pharm, Saarbrücken, Germany) without general anaesthesia. Ten tonometer readings with a TonoLab (Icare, Finland) device were taken directly from the instrument display for each eye measurement, recorded and averaged. "Off" (or outlier) readings and instrument-generated averages were ignored. The IOP appeared to have increased 10 days after cauterization, and it remained elevated for the entire duration of the experiment. Animals in which the IOP returned to normal

levels were discarded ($n = 4$). None of the animals exhibited an enlarged globe or oedematous cornea.

Preparation, dissection and cultivation of the retina

For further analysis of the retina, the rats were killed using an atmosphere of CO_2. Briefly, the eyecups were removed and placed in Hank's balanced salt solution pH 7.4, where all subsequent preparation steps were conducted under sterile conditions. Retina was isolated, flat-mounted on a nitrocellulose filter with fine forceps, divided into eight wedge-shaped pieces and stored under –80° or cultured. Therefore, the retina was placed with the ganglion cell layer on a cell plate. S4 growth medium containing 1% gentamicin was added (3 ml). Cultures were maintained for 96 hr at 37°C in a humidified atmosphere containing 5% CO_2 (Prokosch et al. 2010).

Preparation and primary culture of rat brain microvessel endothelial cells

The brain microvessel endothelial cells of rats (rBMECs) were isolated. All procedures were carried out under aseptic conditions. The brains were removed after decapitation from male and female pups from the Sprague Dawley strain at postnatal days P5 to P8. The brains were immediately placed into ice-cold phosphate-buffered saline (PBS) Connective tissue and meninges were discarded. Cortex grey matter was minced into small, homogenous fragments made by crosscutting the tissue with scalpels. The tissue fragments were suspended and incubated in 10 ml PBS containing 0.05% trypsin for 25 min at 37°C. After incubation, cells were pelleted by centrifugation at 800 ***g*** for 5 min. The pellet was resuspended in 5 ml PBS containing 20% BSA. After centrifugation at 2000 ***g*** for 5 min fat, cell debris and myelin were floating on the aqueous BSA phase. These and the aqueous phase were removed and discarded. The pellet containing the microvessels was resuspended in 2 ml PBS containing 0.1% collagenase A and incubated at 37°C for 30 min. The microvessel endothelial cells were finally collected by centrifugation at 800 ***g*** for 5 min., washed two times in PBS, resuspended in DMEM/F12 supplemented with 20% FCS, 15 mM HEPES and 1% penicillin/streptomycin and cultured at 37°C in 5% CO_2 humidified atmosphere. The medium was changed every 3 days. Before use, cell culture flasks and dishes were gelatinated with 0.5% gelatin for 30 min at 37°C and subsequently let them dry for 10 min at room temperature. For incubation in the pressure chambers, only confluent primary cultures were used.

High-pressure incubation chamber

A metallic incubation chamber was self-fabricated from steel. The metallic high-pressure incubator fabricated to this purpose with screw able cover and unidirected valve to allow for entrance of incubator air. The intracameral air pressure is adjusted with a nanometre with readings in mmHg. Constant air pressure can be obtained over several days. The incubator allowed for increasing the air pressure up to 200 mmHg (266.64 pascal) keeping this pressure stable or changing the pressure on demand. A valve allowed for entrance of 5% CO_2 containing atmosphere from the main incubator (Heraeus, Germany). A pressure gauge was used to continually monitor the air pressure within the high-pressure incubator. Brain cells prepared or retinal explants as described above were cultured for 96 hr within the high-pressure incubator until they were processed for either immunohistochemistry (IHC), Western blotting or qRT-PCR.

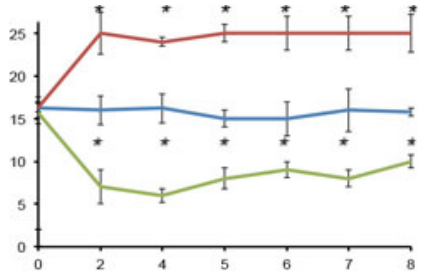

Fig. 1. Follow-up of the IOP in rats after cauterization with elevated IOP (red) and after sectorial iridectomy (green) compared with control normotensive animals (blue) over 8 weeks. IOP was significantly increased throughout the whole follow-up by cauterization and decreased by iridectomy. (*$p < 0.05$). IOP = intraocular pressure.

Western blotting

Cultured cells were treated with trypsin, collected by centrifugation and washed two times with PBS. The samples were processed for Western blotting according to standardized procedures. Briefly, the probes were homogenized in lysis buffer (10 mM Tris pH 7.5, 150 mM natrium chloride, 1 mM EDTA, 1%

Table 1. List of primers and sequences used

Primer	rTGFb2Rez-477F TGF-beta 2; Tgfbr2T TGF-beta 2; Tgfbr2T	Sequence	ATCTGTGAGAAGCCGCAGGA
	rTGFb2Rez-557R TGF-beta 2; Tgfbr2T TGF-beta 2; Tgfbr2T		GTGGCAAACGGTCTCCAGAG
Primer	rB3TUBULIN-F-16 beta 3 class III (Tubb3); MARC_24021-24022:1029778648:1 beta 3 class III (Tubb3); MARC_24021-24022:1029778648:1	Sequence	CCTGCCTCTTCGTCTCTAGC
	rB3TUBULIN-R-114 beta 3 class III (Tubb3); MARC_24021-24022:1029778648:1 beta 3 class III (Tubb3); MARC_24021-24022:1029778648:1		TCCCAGAACTTGGCCCCTAT
Primer	rERK2-MAPK1-F1249 MAPK; Erk2 MAPK; Erk2	Sequence	ATTGGTCAGGACAAGGGCTC
	rERK2-MAPK1-R1373 MAPK; Erk2 MAPK; Erk2		GGAACGGCTCAAAGGAGTCA
Primer	rMAPK3-ERK1-F970 Erk-1; ERK1; ERT2; Esrk1; MAPK1; MNK1; p44; p44erk1; p44mapk; Prkm3; MAPK3 Erk-1; ERK1; ERT2; Esrk1; MAPK1; MNK1; p44; p44erk1; p44mapk; Prkm3; MAPK3	Sequence	CCAAACAAGCGCATCACAGT
	rMAPK3-ERK1-R1051 Erk-1; ERK1; ERT2; Esrk1; MAPK1; MNK1; p44; p44erk1; p44mapk; Prkm3; MAPK3 Erk-1; ERK1; ERT2; Esrk1; MAPK1; MNK1; p44; p44erk1; p44mapk; Prkm3; MAPK3		CCACTGGTTCATCTGTCGGA
Primer	rCDC42-F549 Cdc42 Cdc42	Sequence	CCCTCACACAGAAAGGCCTAA
	rCDC42-R653 Cdc42 Cdc42		GCGTTCATAGCAGCACACAC

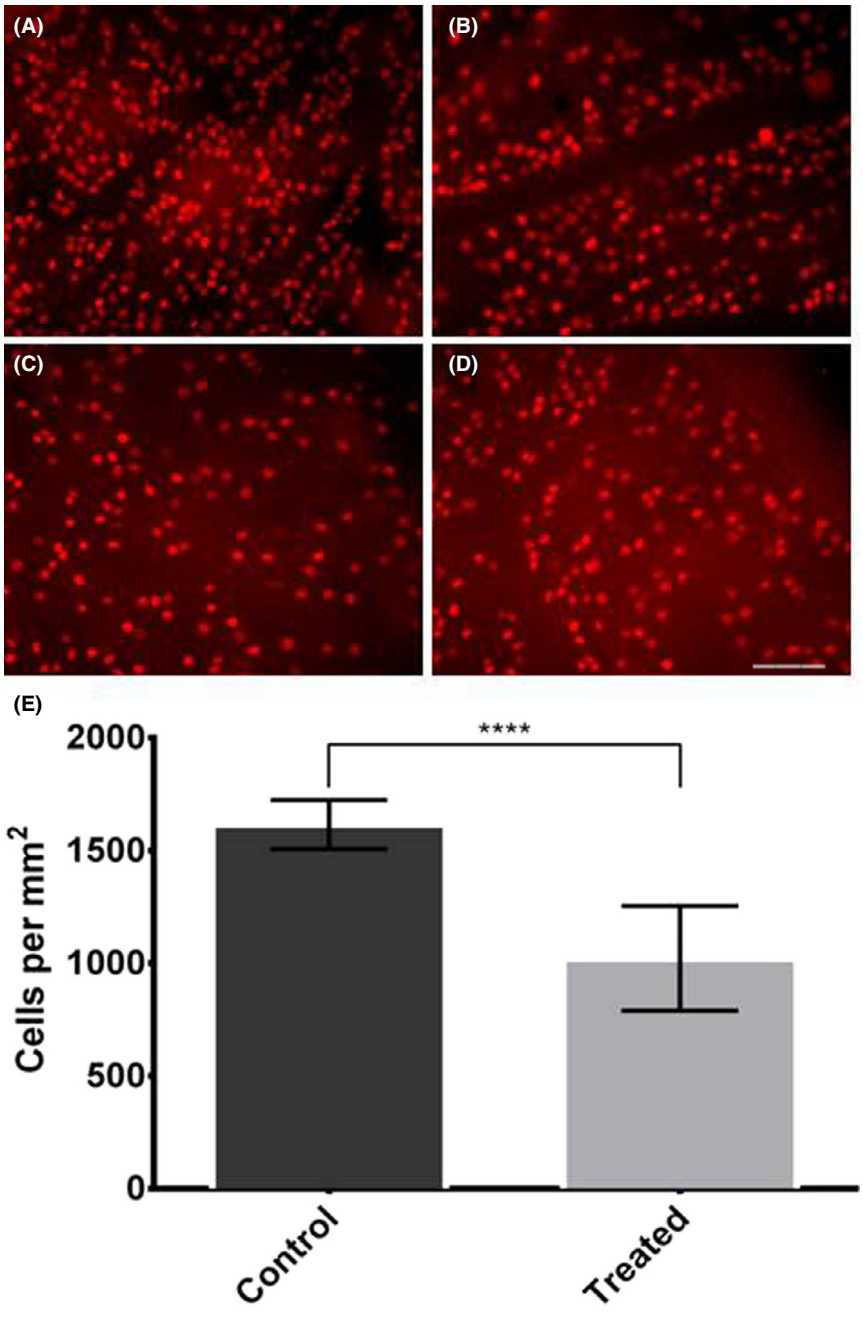

Fig. 2. Number of retinal ganglion cells stained with Brn3a as the primary antibody in retinal whole mounts of control retinae (A, B) and in hypertensive retinas (C, D), showing a significant decrease (****$p < 0.001$) after 8 weeks of elevated intraocular pressure as shown in the graph (E). Scale bar 100 μm.

NP-40, 0.5% NaDoc and 0.25% SDS) and sonicated. Cell debris was removed by centrifugation at 15 000 ***g*** at 4°C for 30 min. The protein concentration was determined using Bradford reagents. Thirty micrograms of protein was electrophoresed on SDS polyacrylamide gels and transferred to a nitrocellulose membrane. The blots were incubated in blocking solution (5% fat-free dry milk in TBS pH7, 6) for 1 hr, followed by incubation overnight at 4°C with anti-beta-III-tubulin (Covance MMS-435P, 1:1000, Münster, Germany), anti-Endothelin 1 (Sigma-Aldrich A1645, 1:1000, Taufkirchen, Germany), anti Rac/cdc42 (Biovision 3080-100, 1:1000, Mainz, Germany), anti ERK 1/2 (Cell Signalling 4695, 1:1000, Biovision Mainz, Germany) and anti-pERK 1/2 (Cell Signalling 4370, 1:1000). The applied control antibodies, anti-calnexin (Sigma-Aldrich C4731), anti-actin (Sigma-Aldrich A5441) and anti-GAPDH (Sigma-Aldrich G9545), were used, at a dilution of 1:10 000, 1:10 000 and 1:100 000, respectively. The membrane was then incubated with the secondary anti-mouse or anti-rabbit antibody conjugated with horseradish peroxidase (Sigma-Aldrich A3682, A9169 1:40 000, cell signalling 7076, 7074 1:5000) in blocking solution for 1 hr at room temperature. Antibody detection was performed with enhanced chemiluminescence (Amersham Biosciences, Rockville, MD, USA). The relative densities of the protein spots were analysed using Alpha Ease (Alpha Ease FC software 4.0, Alpha Innotech, Biozym Scientific, Vienna, Austria). The protein density of a fixed area was determined for each spot after subtracting the specific background density of the same area. The spot density was correlated and normalized to the relative density of the particular application control. The normotensive spot density was defined as the reference mark, and the relative relationships were determined and processed.

Mass spectrometry analysis

For proteomic analysis, the retina was explanted and dissociated using liquid nitrogen and a mortar. Samples from different eyes and animals were collected and treated separately with lysis buffer containing 0.5% n-Dodecyl β-D-maltoside in Tris-buffered saline. Furthermore, the tissue was processed with an ultrasonic bath and ultrasonic wand for efficient cell breakdown. After multiple centrifugation steps, protein concentration was determined by BCA Pierce Protein Assay kit.

SDS-PAGE separation and in-gel digestion

To separate the proteome and facilitate a downstream MS analysis, 60 μg protein mixture per retina sample was added to one gel lane of a NuPage Novex 12% Bis-Tris Protein Gel and SDS-PAGE was performed accordingly. Every gel lane was cut into 17 pieces, de-stained with de-staining buffer (50% 100 mM ammonium bicarbonate in water, 50% acetonitrile) and digested with sequencing grade modified trypsin (Promega) overnight. Finally, the remaining gel pieces were treated with extraction buffer (66% acetonitrile, 32.4% water and 1.6%

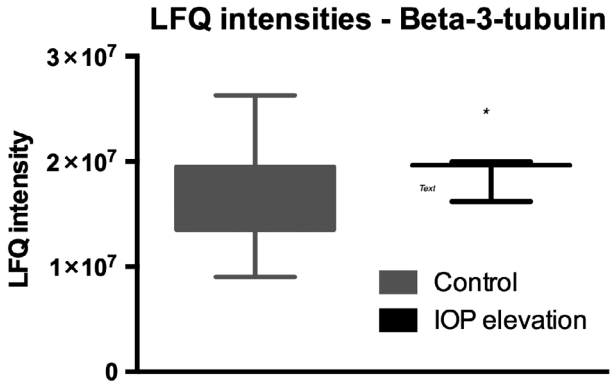

Fig. 3. ß-III-tubulin showed a significant ($p < 0.001$) 1.1-fold increase in hypertensive retinas as measured by mass spectrometry. The graph is showing the label-free quantification (LFQ) intensities.

formic acid) for 30 min and dried in a concentrator. C-18 ZipTips (Millipore, Billerica, MA, USA) were used to clean the samples and separate the peptides from salts and other by-products. Clean samples were stored at –80°C until the mass spectrometric analysis.

LC-ESI/MS protein identification

Peptides from the trypsin in-gel digestion were analysed with a capillary LC-ESI-MS system consisting of a C-18 precolumn and a C-18 analytical column to ensure a resolution during MS measurement. As solvent delivery system, a Rheos Allegro HPLC Pump was used with a 50-min linear gradient system: running buffer A: 98% H_2O, 1.94% ACN, 0.06% methanol and 0.05% TFA and running buffer B: 95% ACN, 3% methanol, 1.95% H_2O and 0.05% TFA. (0–2 min: 85% A, 15%B; 2–35 min: 80% A, 20% B; 35–40 min: 40% A, 60% B; 40–50 min: 100% A). Mass spectra were obtained using an LTQ OrbitrapXL. The full-scan mass spectra (m/z 300–2000) were acquired with a resolution of 30.000.

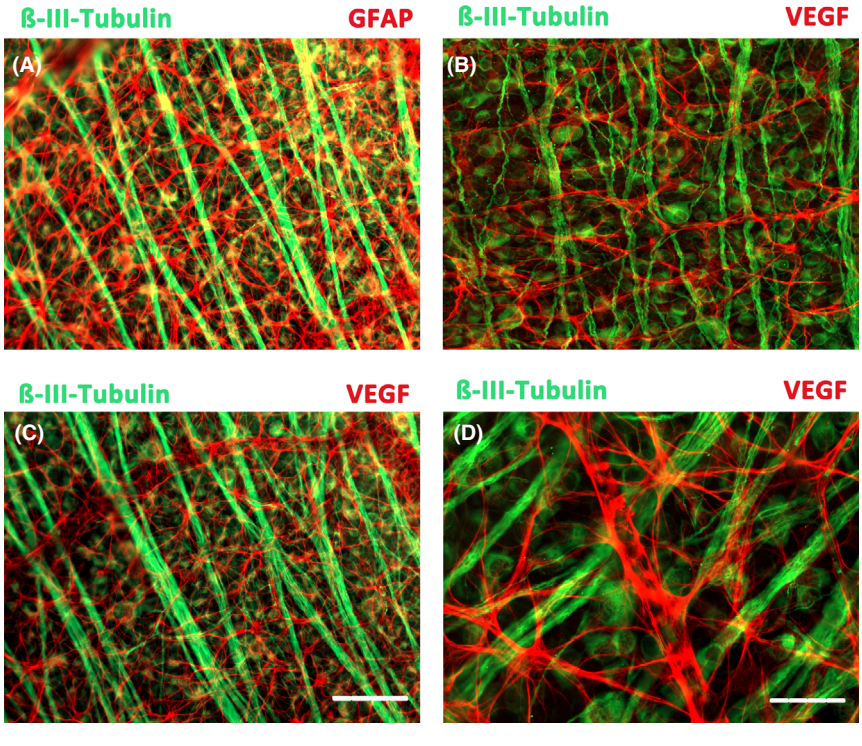

Fig. 4. ß-III-tubulin expression in the normal rat retina in vivo. Double staining with glial fibrillary protein (astrocytes) and ß-III-tubulin (RGCs) in the normal retina (A). Staining of RGC axon bundles and cell bodies with ß-III-tubulin in normotensive whole mounts, and VEGF staining of perivascular astrocytes (B, C). Higher magnification showing the district staining of ß-III-tubulin in RGCs and axons, with no vessels and astrocytes remaining only VEGF-positive (D). Scale bars 50 µm in A–C, 25 µm in D. RGC = retinal ganglion cell.

Data processing

Subsequently, mass spectra were analysed in terms of protein identification and quantification using Maxquant. Fixed protein modifications were set to oxidation and acetylation. The match tolerance in mass precision for MS/MS was adjusted to 20 ppm and 0.5 Da. The false discovery rate for proteins and peptides was set at 0.01, the minimum peptide length was six amino acids, and the minimum unique peptides were set at 0 (razor peptides at 1).

IHC – RGCs and retinal explants

Immunohistochemistry (IHC) was also performed in retinal whole mounts obtained from the in vivo groups and explants after cultivation. Briefly, the tissue was fixed in 4% paraformaldehyde for 1 hr, washed twice in PBS and stored over 24 hr in 30% sucrose solution in PBS, pH 7.4 at 4°C. Then, the specimens were washed in PBS and rapidly frozen in *N*-methyl-butan/liquid nitrogen and transferred into PBS for immunohistochemical processing. Incubation with a primary antibody anti-BRN3A, anti-endothelin or anti ß-III-tubulin antibody as listed for Western blotting was done in 0.5% Triton-X containing PBS over 3 days at 4°C. After washing in PBS (3 times, 30 min each), the secondary antibody was incubated in 0.5% Triton-X containing PBS over 3 days at 4°C. The nuclei of retinal cells were stained by adding 4′,6-diamino-2-phenylindole dihydrochloride hydrate (DAPI, Sigma-Aldrich). After washing in PBS (overnight at 4°C), the whole mounts were embedded in Mowiol and cover-slipped for fluorescence microscopy (Axio-Imager M2; Carl Zeiss, Jena, Germany) with the appropriate filters. Negative controls comprised sections processed without addition of the primary antibodies. Control and experimental sections were stained simultaneously to avoid variations in immunohistochemical staining.

Brain microvessel endothelial cells of rats cultured on gelatinated coverslips were prepared for IHC as follows. The specimens were washed 10 min with

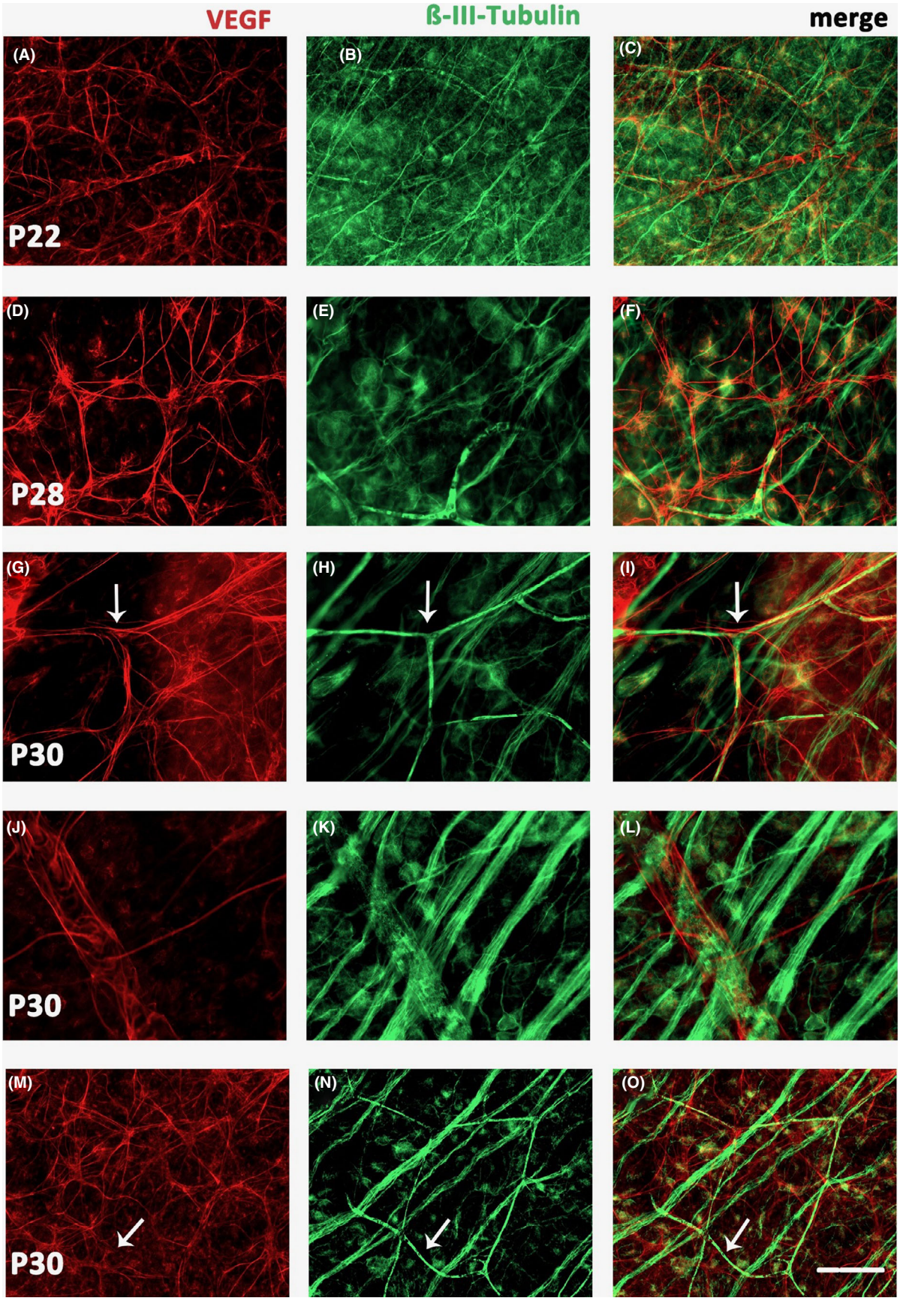

Fig. 5. Double staining of retinal whole mounts with VEGF (red) and ß-III-tubulin (green). In hypertensive retinas, VEGF-positive astrocytes wrapped the vessel walls (A, D, G, J, M), while ß-III-tubulin stained both the RGCs and their axons, in addition to blood capillaries and vessels indicated by arrows in C, H, I, M, N, and O. The IOP (P22-30) is exemplarily indicated in each of the six experimental retinas by a pin. Scale bar 50 µm.

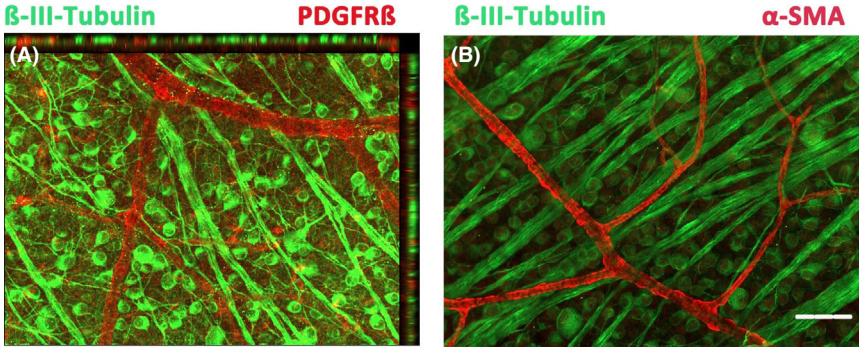

Fig. 6. Expression of markers in the normotensive retina. (A) Double staining with the pericyte marker PDGFR-ß and ß-III-tubulin. (B) Double staining with α-SMA and ß-III-tubulin. Scale bar 50 μm.

PBS, fixed in 4% paraformaldehyde for 10 min and washed 10 min with PBS. The coverslips were blocked with 10% FCS containing 0.0025 vol.% Triton-X-100 for 1–2 hr at RT. Incubation with the first antibody diluted in 10% FCS was carried out overnight at 4°C. Specimens were washed two times with PBS for 15 min., blocked again with 10% FCS containing 0.0025 vol.% Triton-X-100 for 30 min at RT and incubated with the secondary antibody for 2 hr at RT. Finally, the coverslips were embedded with DAPI-Mowiol on glass slides and examined with a fluorescence microscope as mentioned above.

Quantitative real-time polymerase chain reaction

The real-time PCR was implemented in an ABI PRISM 7900 sequence detector (Applied Biosystems) in 384-well plates. For the qRT-PCR, total RNA was isolated from the cultured rBMECS and from the retinas of a second set of animals, because there was insufficient RNA from the microarray experiments for both experiments. Five rats with IOP elevation and five animals with a normal IOP were used for qRT-PCR experiments. One microgram of total RNA was first reverse transcribed using the Omniscript Reverse Transcriptase (5 mM dNTPs, 10 × RT buffer, 10 units/μl RNase inhibitor and 10 μM Oligo-dT primer; MWG Biotech) in a total volume of 20 μl for 1 hr at 37°C. The enzyme was inactivated by heating at 95°C for 5 min. The cDNA was diluted twofold, and a 1-μl aliquot was used for each 20-μl PCR using the Power SYBR Green PCR Master Mix (Applied Biosystems). Forward and reverse primers were designed for the detection and quantitation of specific rat genetic sequences in RNA samples converted to cDNA. The reaction components consisted of 10 μl of Power SYBR Green PCR Master Mix, 0.14 μl forward and reverse primer and 1 μl of cDNA in a 20-μl reaction. The PCR conditions for all genes were as follows: initial denaturation 10 min 95°C, 40 cycles of denaturation (15 seconds, 95°C), annealing and extension (1 min 60°C). Each sample was run in duplicate. The data were analysed using Step one Plus Real-Time PCR software (Applied Biosystems). GAPDH served as the endogenous control against which to normalize the amount of cDNA added to each reaction (ΔC_t), and the mean ΔC_t of control samples was used as the calibrator to calculate $\Delta\Delta C_t$. The comparative C_t method was employed, whereby the relative quantity of the respective target gene mRNA – normalized to the endogenous control and relative to the calibrator – is expressed as the relative change: $2^{-\Delta\Delta C_t}$. The primers used are shown in Table 1.

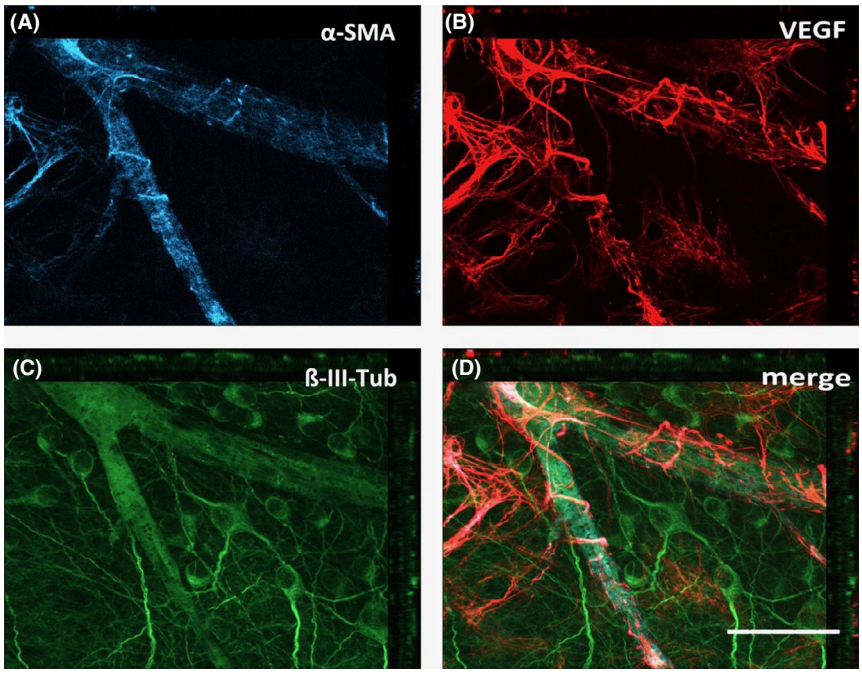

Fig. 7. Triple staining showing the expressions of α-SMA (A), VEGF (B) and ß-III-tubulin (C) along a bifurcation of a retinal vessel in the hypertensive retina. Note the strong expression of ß-III-tubulin in RGCs and the retinal vessel (C, D) that is colocalized with pericytes (α-SMA-positive) and astrocytes (VEGF-positive). Scale bar 25 μm.

Statistical analysis

All data regarding IOP recordings, RGC densities of retinal whole mounts and relative protein densities in WBs are presented as mean ± SD values. Data were analysed statistically using the two-independent samples test (SPPS, Statistica version 7) for Gaussian distributions, with the remaining quantitative data analysed using two-way analysis of variance (Statistica version 7) with post hoc analyses using the Tukey HSD test to identify possible differences among the experimental groups. If the distribution was not Gaussian, the Kruskal–Wallis H test was used.

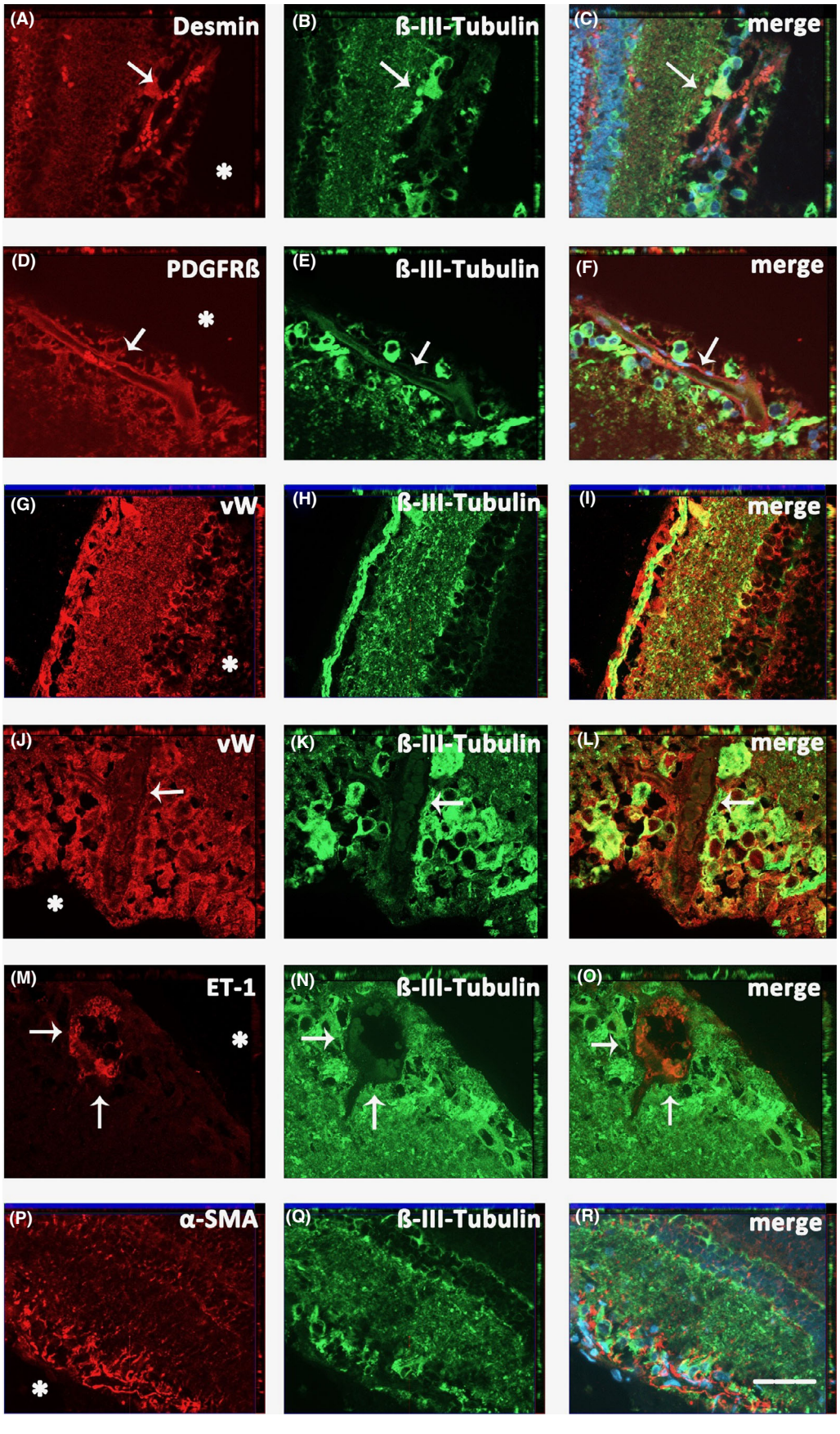

Fig. 8. Colocalization of ß-III-tubulin with different endothelial cell and pericyte markers (some examples indicated by arrows) seen in sections through the hypertensive retina. (A–C) Desmin and ß-III-tubulin, (D–F) PDGFRß and ß-III-tubulin, (G–L) von Willebrand factor and ß-III-tubulin, (M–O) ET-1 and ß-III-tubulin, (P–R) α-SMA and ß-III-tubulin. Asterisk in each lane indicates the vitreous body adjacent to the RGC layer. Colocalization of ET-1 and ß-III-tubulin could not be remarkably shown. Scale bar: 25 µm.

Results

ß-III-tubulin *in vivo*

The initial experiments consisted of increasing or decreasing the IOP in adult rat eyes in order to examine retinal responses. It appeared that cauterization of the episcleral veins induced an increase in IOP at levels of about 25 mmHg over 8 weeks of postsurgery monitoring. In contrast, sectorial iridectomy reduced the IOP to levels of about 7 mmHg over the same time of monitoring (Fig. 1). There was a significant ($p < 0.001$) decrease in around 20% in RGCs in eyes with elevated IOP (1114 ± 47.2 RGC/mm^2) compared with normal controls (1390 ± 38.6 RGC/mm^2) (Fig. 2A–E). To identify candidate molecules regulated during retina exposure to either hyper- or hypotensive intraocular conditions, the retinas were excised and examined with mass spectrometry and IHC. ß-III-tubulin showed a significant ($p < 0.001$) 1.1-fold increase in hypertensive retinas, although RGCs exclusively expressing ß-III-tubulin showed a 20% decrease (Fig. 3). Thus, we further examined retinal whole mounts by IHC looking for cells abnormally expressing ß-III-tubulin.

In adult untreated rat retinas, β-III-tubulin was exclusively expressed in RGCs and their axons bundles in all areas of the retina (Fig. 4A). Retinal astrocytes expressed glial fibrillary protein but remained negative for ß-III-tubulin staining (Fig. 4A). When double stained with vascular endothelial growth factor (VEGF) to outline perivascular astrocytes, β-III-tubulin-stained RGCs were surrounded by a VEGF-positive astrocytic network (Fig. 4B). The VEGF-positive perivascular astrocytes and the ß-III-tubulin-positive RGCs were easily discernible at higher magnifications (Fig 4C,D). No β-III-tubulin-positive astrocytes or vascular or perivascular cells were observed in the untreated retinas. When double stained with VEGF, β-III-tubulin-stained RGCs were surrounded by the VEGF-positive astrocytic network and Müller cell end feet (Fig. 4A,C,E). No β-III-tubulin-positive vascular or perivascular cells were observed in the untreated retinas.

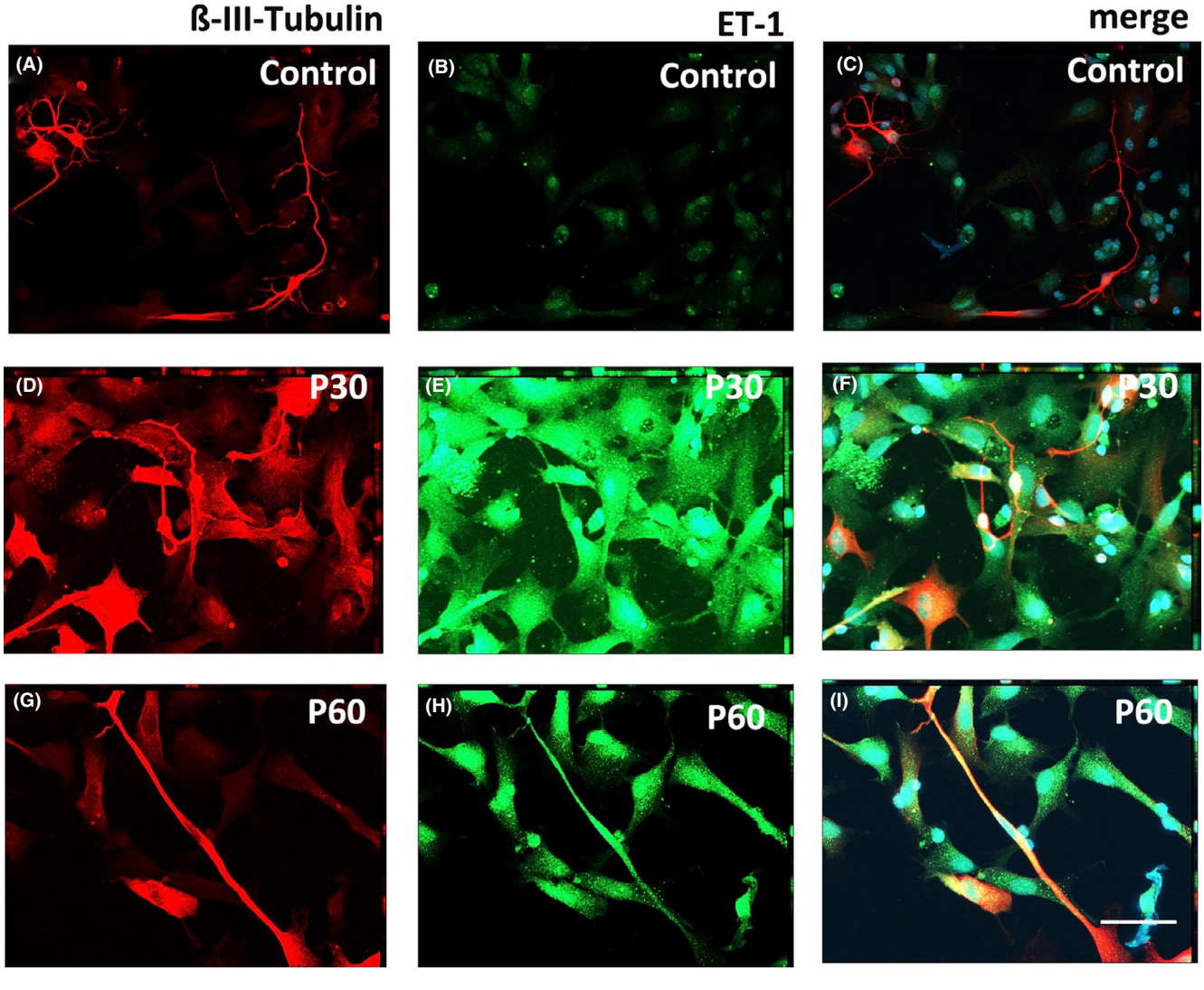

Fig. 9. Expression of ß-III-tubulin in rRMECs. (A–C) Double staining with ß-III-tubulin (A) and ET-1 (B) in cells cultured without elevated air pressure shows no colabelled cells (C). (D–F) Same IHC arrangement of cells cultured at 30 mmHg clearly shows increased labelling for ß-III-tubulin and colabelling with ET-1. (G–I) Same IHC arrangement of cells cultured at 60 mmHg shows expression of ß-III-tubulin in ET-1-positive cells. Scale bar: 25 μm.

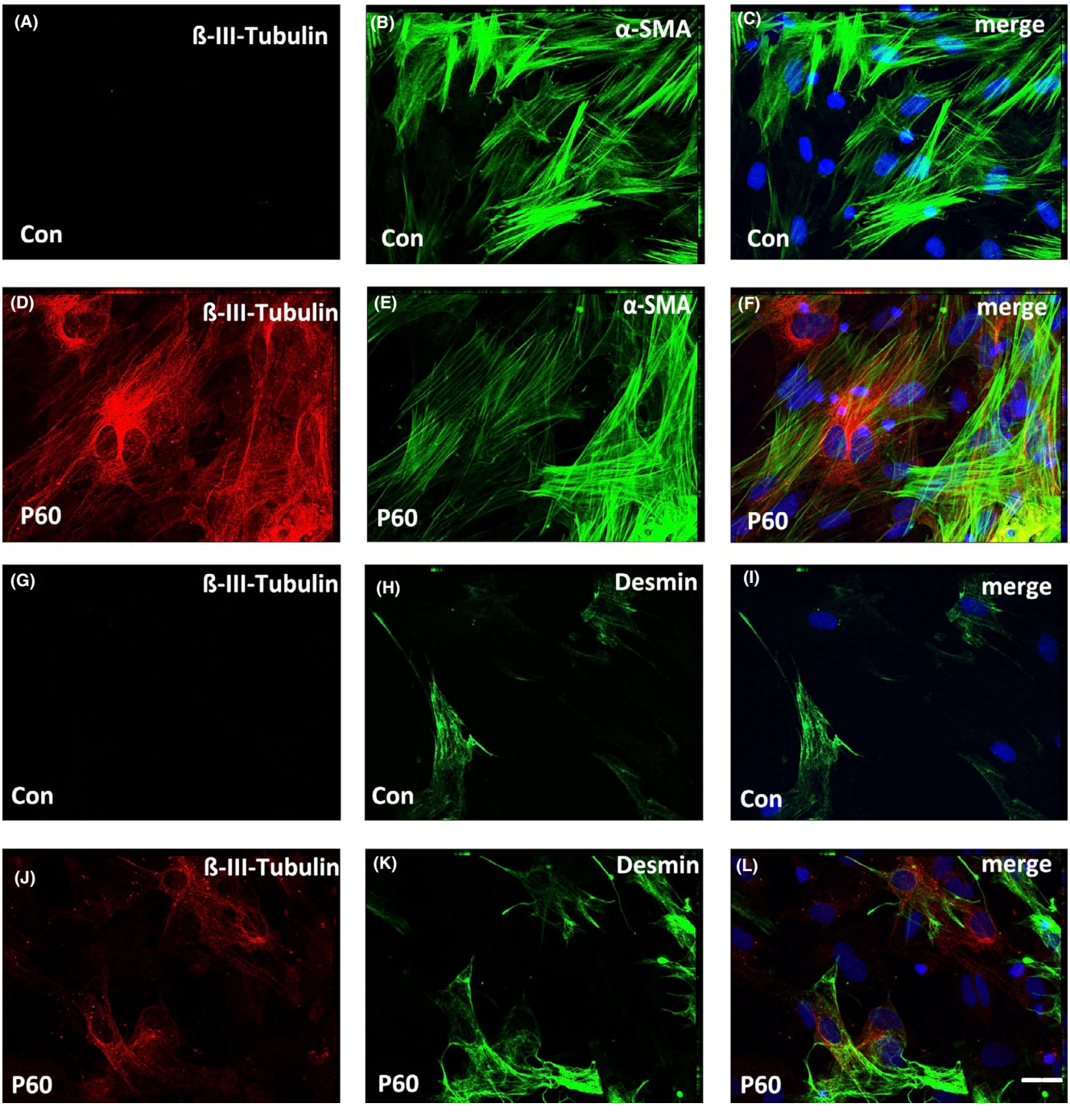

Fig. 10. Expression of β-III-tubulin in rBMECs. (A–C) Double staining with ß-III-tubulin A) and α-SMA (B) in cells cultured without elevated air pressure shows no colabelled cells (C). (D–F) Same IHC arrangement of cells cultured at 60 mmHg clearly shows increased labelling for ß- III-tubulin and colabelling with α-SMA. (G–I) Same IHC arrangement of control cells showed no expression of ß-III-tubulin. (J–L) An increased pressure of 60 mmHg also resulted in staining of pericytes with desmin. Scale bar: 25 μm.

We then studied the expression of β-III-tubulin in retinas exposed to IOP elevation. The β-III- tubulin labelling was spatially correlated with the locations of vessel walls (Fig. 5), but it always appeared outside the VEGF-positive astrocytes, giving the impression of been localized along pericytes, endothelial cells or both cell types. When double labelled with VEGF, there was a strong distinction between the labelled structures with the astrocytic processes to wrap the β-III-tubulin vascular labelling in hypertensive retinas (Fig. 5). We next re-examined the expression of different markers in capillaries and ß-III-tubulin in the normotensive retina to assess whether ß-III-tubulin was expressed in capillaries. It appeared that α-SMA (Fig. 6) and PDGFR-ß (Fig. 6A) only outlined capillaries and vessels, without being colocalized with ß-III-tubulin that appeared positive only in RGCs and axons (Fig. 6A,B). In contrast, the hypertensive retina showed staining of α-SMA (pericytes) and VEGF (astrocytes), with ß-III-tubulin staining of the RGCs and blood vessels, indicating a changed expression of the neuron-

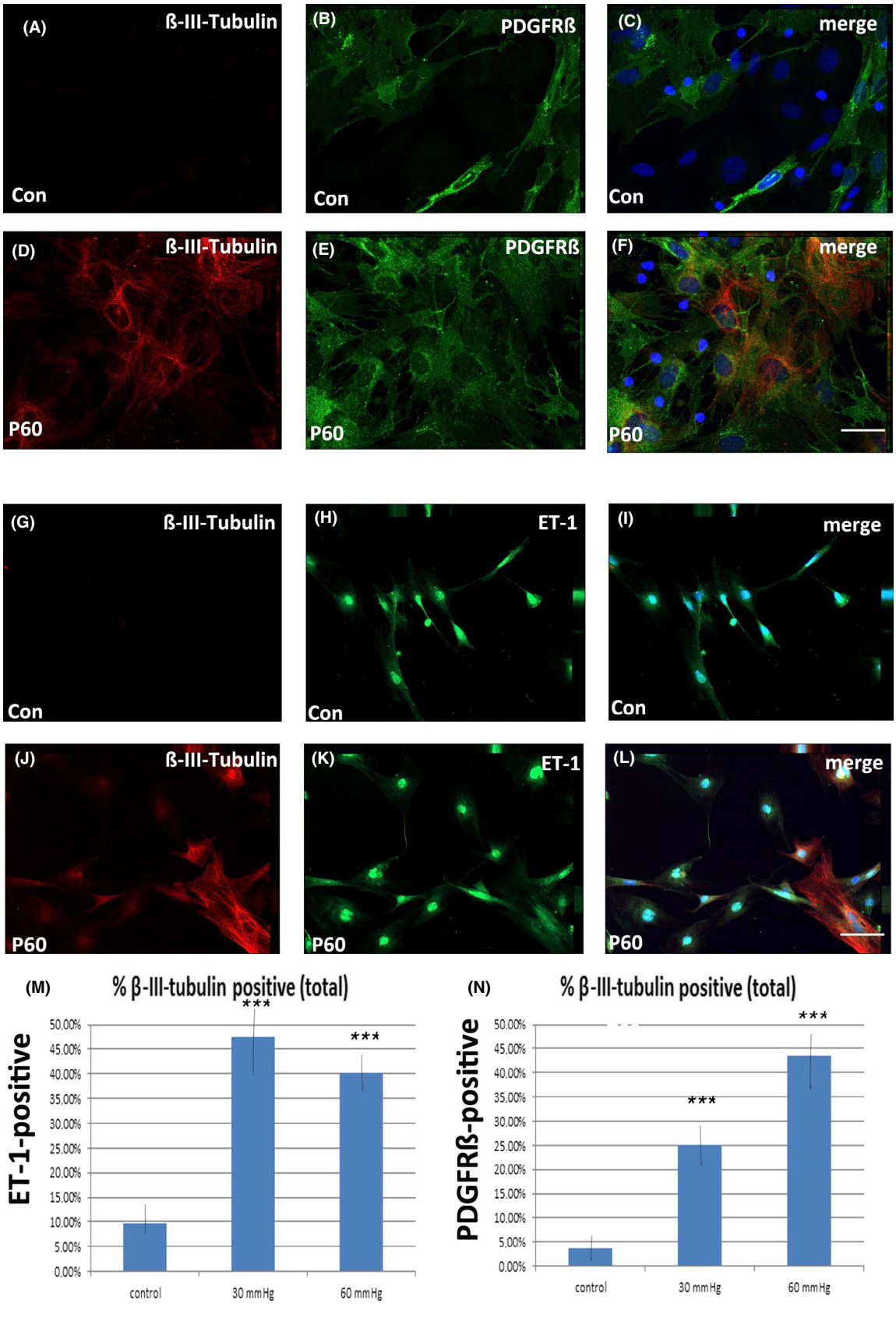

Fig. 11. Expression of ß-III-tubulin (red) in rBMECs and α-SMA (green)-positive pericytes. Nuclei are stained with DAPI (A, B). Double staining with ß-III-tubulin (A) and PDGFR-β (B) in cells cultured without elevated air pressure shows no colabelled cells and no ß-III-tubulin positive cells (A–C). (D–F) Same IHC arrangement of cells cultured at 60 mmHg clearly shows increased labelling for ß-III-tubulin and colabelling with PDGFR-β-positive pericytes. (G–I) Same IHC arrangement of cells colabelled with a marker for endothelial cells (i.e., ET-1). (M) Counts of β-III-tubulin-positive cells for the cultures shown in G–L. Data are shown as ±SD. (***$p < 0.001$). Scale bar: 25 µm.

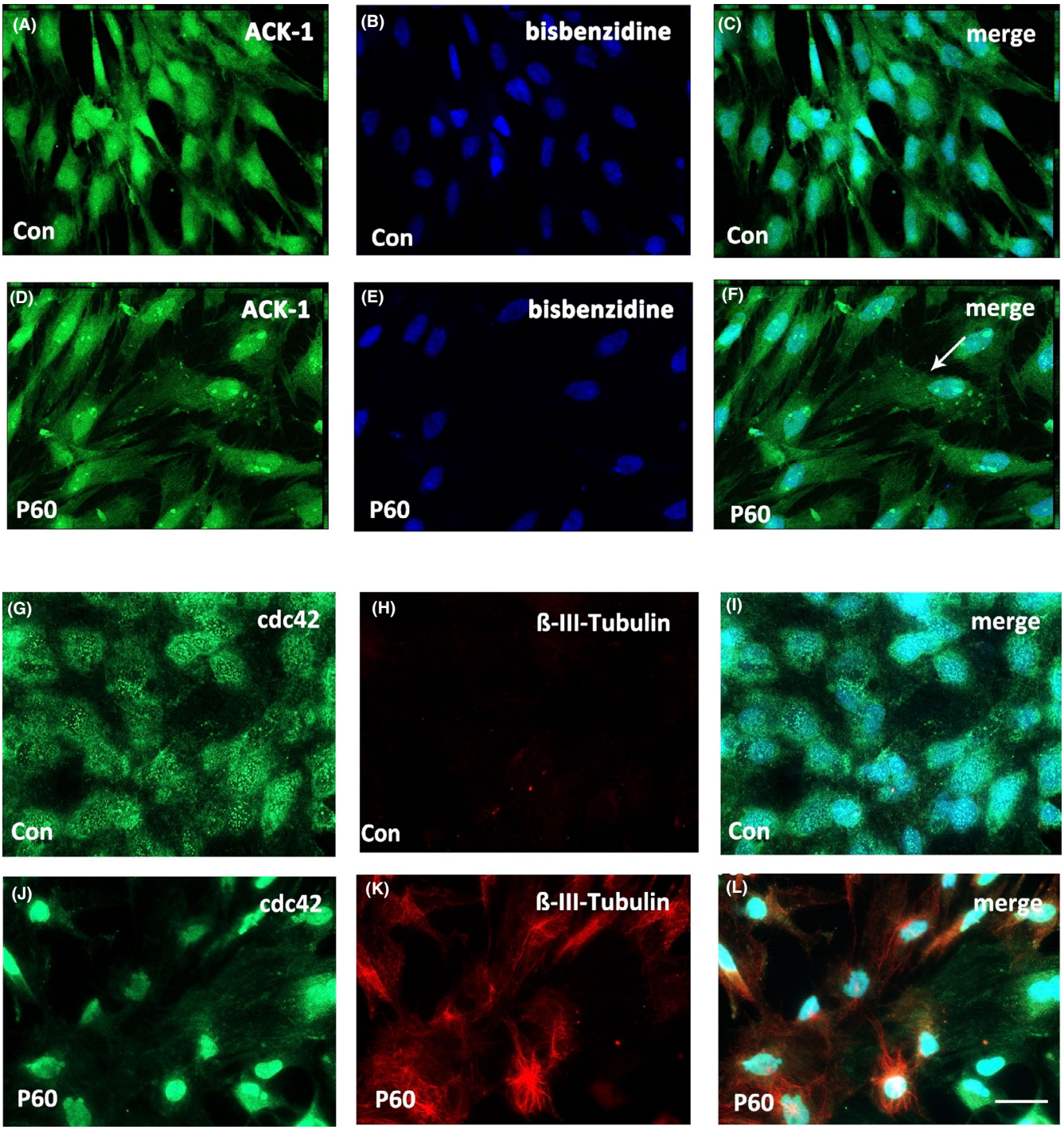

Fig. 12. Cell signalling. Expression of ACK-1 in cultured rBMECs under control conditions (A–C) and under the high pressure of 60 mmHg. Note that ACK-1 appears aggregated with the cytoplasm in cells at 60 mmHg (D–F). The cell indicated by an arrow in F is shown enlarged in O to outline the aggregates. In contrast, cdc42 remained unchanged in the cells cultured under control conditions (G–I). On the other hand, increasing the air pressure to 60 mmHg (J–L) up-regulated ß-III-tubulin (K, L) and reduced cdc2 expression compared to controls (L).

specific marker in blood vessels (Fig. 7C,D). These data indicate that ß-III-tubulin is expressed in RGCs and capillaries in hypertensive retinas.

We next examined the topological relationship of different capillary markers to ß-III-tubulin in hypertensive retina sections, which revealed a strong colocalization with desmin, PDGFR ß, von Willebrand factor, ET-1 and α-SMA (Fig. 8). These data confirmed that both endothelial cells (ET-1) and pericytes (α-SMA- and PDGFR-ß positive) express ß-III-tubulin as a response to IOP elevation (Fig. 8).

ß-III-tubulin in vitro

In order to verify whether ß-III-tubulin is also expressed in cultured retinal cells, rRMECs were cultured either under normal incubator conditions (controls) or in an elevated air pressure condition of either 30 mmHg or 60 mmHg in vitro. After 3 days, IHC staining

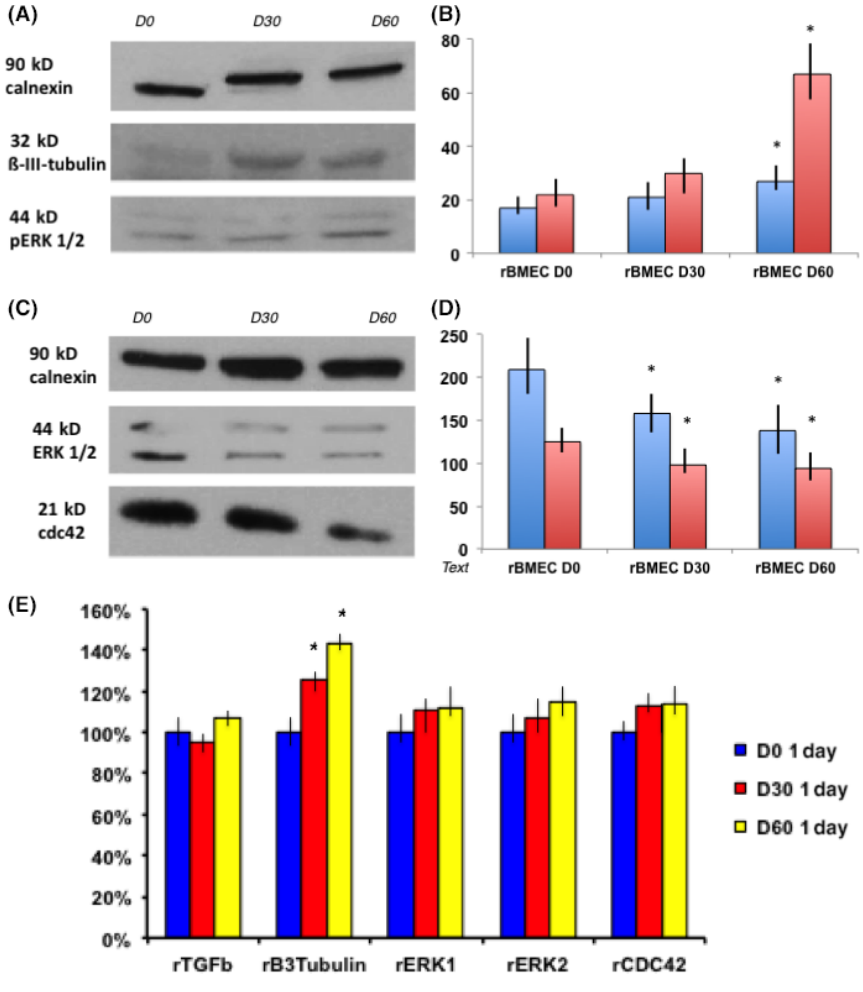

Fig. 13. Signalling associated with β-III-tubulin in primary rBMECs exposed to high air pressure. (A, B) ß-III- tubulin (blue in the graph) and pERK1/2 (red) increase in rBMECs cultured at 30 mmHg (D30) and 60 mmHg (D60). The difference is significant * for both markers at 60 mmHg. (C, D) Under the same culture conditions, ERK 1/2 (blue) decreased significantly at 30 and 60 mmHg. In addition, cdc42/Rac (blue) decreased significantly both at 30 and 60 mmHg. qRT- PCR data could not confirm the results as PCR data were not significantly changed (E). *$p < 0.05$. Data are shown as –/–SD by the bar.

was evident in the RGCs of controls (Fig. 9A–C). In contrast, some typical ET-1-positive endothelial cells also stained positive for ß-III-tubulin (Fig. 9D–I). These data indicate that retinal endothelial cells responded to pressure elevation with the expression of ß-III-tubulin. To expand on β-III-261 tubulin expression in vitro, primary microvessel endothelial cells were created from rat brains and cultured under identical conditions as for the retinal cells. The rationale for using single brain cells was that such cells are exposed to air pressure from all directions, resembling in vivo IOP. Cultured primary BMECs and pericytes did not express β-III-tubulin under normotensive culture conditions in vitro (Fig. 10A–C). In contrast, these cells coexpressed α-SMA plus β-III-tubulin depending on the air pressure: increasing the pressure from 30 mmHg (not shown) to 60 mmHg (Fig. 10D–F) was associated with an increasing proportion of β-III-positive endothelial cells. Similar results were obtained with a second marker for pericytes (desmin), verifying that the cells express β-III-tubulin under high pressure (Fig. 10G–L). Further verification and quantification were performed using double staining with PDGFR-β and β-III-tubulin (Fig. 11A–F) or ET-1 and β-III-tubulin (Fig. 11G–L). Cell counts revealed that 9.8%, 47.42% and 40.26% of all ET-1-positive cells under control, 30- mmHg and 60-mmHg conditions, respectively, coexpressed ß-III-tubulin (Fig. 11M). Analogously, 4% of α-SMA cells coexpressed ß-III-tubulin in controls, increasing to 25% at 30 mmHg and 44% at 60 mmHg (Fig. 11N), indicating that almost each second pericyte expressed α-SMA (Fig. 11D–F) under pressure. These data show that a high proportion of capillary cells respond to an elevation of pressure with expression of β-III-tubulin in vitro.

Finally, we studied cell signalling of β-III-tubulin-expressing retinas and rBMECs and analysed cell lysates using IHC and Western blotting for selected intracellular proteins involved in ß-III-tubulin signalling. The kinase ACK-1 was expressed in all cells under normal culture conditions (Fig. 12A–C) and became intracytoplasmically redistributed under high pressure (Fig. 12D–F,O). On the other hand, cdc42 appeared in all cultured cells in the control cultures (Fig. 12G–I), becoming down-regulated in cells cultured under high pressure (Fig. 12J–L). These data were confirmed by Western blotting showing a decrease in cdc42 in the elevated pressure conditions, while pERK1/2 increased (Fig. 13).

It appeared that ß-III-tubulin and pERK 1/2 signalling increased in cells cultured under elevated air pressure, whereas ERK 1/2 signalling (Fig. 13A, B) and cdc42/Rac decreased with increased air pressure (Fig. 13C,D). However, qRT-PCR data did not confirm the results (E), as the PCR data were not significantly changed.

These data indicate that β-III-tubulin expression in elevated pressure conditions influences the ERK1/2 pathway in a specific way.

Discussion

The main finding of this study is that neuron-specific β-III-tubulin is expressed in retinal pericytes and endothelial cells exposed to either elevated IOP in vivo or elevated air pressure within the incubation chamber *in vitro* and *in vivo*. The unprecedented upregulation of β-III-tubulin in non-neuronal cells is likely not associated with ERK 1/2 and cdc42/Rac signalling. Although β-III-tubulin is a constituent of neuronal microtubules and is recognized as a neuronal marker (Sharma & Netland 2007), the protein was also identified as a marker of angiogenic, NG2-positive perivascular cells during remodelling of adult rat mesenteric networks in culture (Stapor & Murfee 2012).

Vascularization is also a critical player in tissue neutrification, oxygenation and integral maintenance. Vascular pericytes

are functionally linked with vascular wall stabilization, regulation of vessel permeability and proliferation of endothelial cells (Ellenius et al. 1997; Hellgren et al. 2016).

Although the functions of pericytes may vary between the different normal tissues and growing tumours, they emerged as a cellular target to suppress angiogenesis during tumour growth (Famiglietti et al. 2003; Ozerdem 2006). However, the pericytes interact with endothelium cells using intercellular signalling governed by Ang-1/Tie2, TGF-β and PDGF-β/PDGFR-β interactions (Folkmann et al. 2012). Here, we showed that both types of interacting vascular cells express the neuronal marker β-III-tubulin under conditions simulating GN. These results suggest that neural and vascular responses to high IOP may involve β-III-tubulin. There are emerging lines of evidence that GN affects primarily the microvasulature at the levels of retina and optic nerve head (Martus et al. 2004). Clinical-ophthalmological signs of such affections are microinfarcts and bleedings at preglaucomatous stages in humans (Martus et al. 2004). However, there are no molecular biomarkers available to examine such changes at cellular and subcellular level in humans. In the rat model of IOP elevation presented here, expression of β-III-tubulin is likely a biomarker of cellular changes occurring both in pericytes and endothelial cells. β-III-tubulin is one of the seven β-III-tubulin isotypes which form αβ-tubulin heterodimers with six α-tubulin isotopes during the assembly of microtubules (Katsetos et al. 2003). In the CNS including the retina, β-III-tubulin is a neuron-specific neuronal developmental marker (Katsetos et al. 2003). This specific expression in neurons indicates that the vascular cell responses we observed here are signs of pathological responses likely associated with a pressure-induced remodelling. It is interesting that the expression in vascular cells was not observed in retinal explants which lacked an intraluminar perfusion in contrast to the retina *in vivo* that was perfused. The absence of vascular perfusion in this culture is just one of the many possible relevant parameters. In fact, the studies on primary cells show that merely applying pressure on vascular cells can induce ß-III-tubulin expression. We do not know why this does not happen when the same pressure is applied to the (cells in the) retinal explants.

Proteins associated with β-III-tubulin expression are also involved in cellular responses to oxidative stress and glucose deprivation (Cicchillitti et al. 2008). It is therefore not surprising that a proteomic analysis of the rat retina exposed to elevated IOP revealed several proteins with association to cellular stress such as heat shock proteins, crystallins, glucose utilizing proteins, peroxiredoxins and a number of enzymes (Prokosch et al. 2010, 2013). Still, specific functions of β-III-tubulin remain to be scrutinized and additional studies will be required to determine its mechanistic role during manifestation of glaucoma.

References

Chauhan BC, Pan J, Archibald ML, LeVatte TL, Kelly ME & Tremblay F (2002): Effect of intraocular pressure on optic disc topography, electroretinography, and axonal loss in a chronic pressure-induced rat model of optic nerve damage. Invest Ophthalmol Vis Sci **43**: 2969–2976.

Cicchillitti L, Penci R, DiMichele M, Filippetti F, Rotilio D, Donati MB, Scambia G & Ferlini C (2008): Proteomic characterization of cytoskeletal and mitochondrial class III beta-tubulin. Mol Cancer Ther **7**: 2070–2079.

Draberova E, Del Valle L, Gordon J et al. (2008): Class III beta-tubulin is constitutively coexpressed with glial fibrillary acidic protein and nestin in midgestational human fetal astrocytes: implications for phenotypic identity. J Neuropathol Exp Neurol **67**: 341–354.

Eisner A, Samples JR, Campbell HM & Cioffi GA (1995): Foveal adaptation abnormalities in early glaucoma. J Opt Soc Am A Opt Image Sci Vis **12**: 2318–2328.

Ellenius J, Groth T & Lindahl B (1997): Neural network analysis of biochemical markers for early assessment of acute myocardial infarction. Stud Health Technol Inform **43**(Pt A): 382–385.

Famiglietti EV, Stopa EG, McGookin ED, Song P, LeBlanc V & Streeten BW (2003): Immunocytochemical localization of vascular endothelial growth factor in neurons and glial cells of human retina. Brain Res **969**: 195–204.

Findl O, Rainer G, Dallinger S et al. (2000): Assessment of optic disk blood flow in patients with open-angle glaucoma. Am J Ophthalmol **130**: 589–596.

Flammer J & Mozaffarieh M (2008): Autoregulation, a balancing act between supply and demand. Can J Ophthalmol **43**: 317–321.

Folkmann JK, Vesterdal LK, Sheykhzade M, Loft S & Moller P (2012): Endothelial dysfunction in normal and prediabetic rats with metabolic syndrome exposed by oral gavage to carbon black nanoparticles. Toxicol Sci **129**: 98–107.

Galassi F, Giambene B & Varriale R (2011): Systemic vascular dysregulation and retrobulbar hemodynamics in normal-tension glaucoma. Invest Ophthalmol Vis Sci **52**: 4467–4471.

Grunwald JE, Piltz J, Hariprasad SM & DuPont J (1998): Optic nerve and choroidal circulation in glaucoma. Invest Ophthalmol Vis Sci **39**: 2329–2336.

Grunwald JE, Riva CE, Stone RA, Keates EU & Petrig BL (1984): Retinal autoregulation in open-angle glaucoma. Ophthalmology **91**: 1690–1694.

Hellgren G, Lofqvist C, Hard AL, Hansen-Pupp I, Gram M, Ley D, Smith LE & Hellstrom A (2016): Serum concentrations of vascular endothelial growth factor in relation to retinopathy of prematurity. Pediatr Res **79**: 70–75.

Kaiser PK (1995): A comparison of pressure patching versus no patching for corneal abrasions due to trauma or foreign body removal. Corneal Abrasion Patching Study Group. Ophthalmology **102**: 1936–1942.

Katsetos CD, Herman MM & Mork SJ (2003): Class III beta-tubulin in human development and cancer. Cell Motil Cytoskelet **55**: 77–96.

Kornzweig AL, Eliasoph I & Feldstein M (1968): Selective atrophy of the radial peripapillary capillaries in chronic glaucoma. Arch Ophthalmol **80**: 696–702.

Leske MC (2007): Open-angle glaucoma – an epidemiologic overview. Ophthalmic Epidemiol **14**: 166–172.

Martus P, Harder B, Budde WM & Jonas JB (2004): [Follow-up examination of eyes with chronic open-angle glaucoma and optic disc hemorrhages]. Ophthalmologe **101**: 505–508.

Michelson G, Groh MJ & Langhans M (1996): Perfusion of the juxtapapillary retina and optic nerve head in acute ocular hypertension. Ger J Ophthalmol **5**: 315–321.

Murfee WL, Skalak TC & Peirce SM (2005): Differential arterial/venous expression of NG2 proteoglycan in perivascular cells along microvessels: identifying a venule-specific phenotype. Microcirculation **12**: 151–160.

Ozerdem U (2006): Targeting pericytes diminishes neovascularization in orthotopic uveal melanoma in nerve/glial antigen 2 proteoglycan knockout mouse. Ophthalmic Res **38**: 251–254.

Ozerdem U & Freeman WR (2001): Exudative retinal detachment following grid laser photocoagulation in a patient with hemiretinal vein occlusion. Eur J Ophthalmol **11**: 89–92.

Peirce SM & Skalak TC (2003): Microvascular remodeling: a complex continuum spanning angiogenesis to arteriogenesis. Microcirculation **10**: 99–111.

Prasanna G, Krishnamoorthy R & Yorio T (2011): Endothelin, astrocytes and glaucoma. Exp Eye Res **93**: 170–177.

Prokosch V, Chiwitt C, Rose K & Thanos S (2010): Deciphering proteins and their functions in the regenerating retina. Expert Rev Proteomics **7**: 775–795.

Prokosch V, Schallenberg M & Thanos S (2013): Crystallins are regulated biomarkers for monitoring topical therapy of glaucomatous optic neuropathy. PLoS One **8**: e49730.

Quigley HA & Broman AT (2006): The number of people with glaucoma worldwide in 2010 and 2020. Br J Ophthalmol **90**: 262–267.

Resch MD, Resch BE, Csizmazia E, Imre L, Nemeth J, Revesz P & Csanyi E (2010): Permeability of human amniotic membrane to ofloxacin in vitro. Invest Ophthalmol Vis Sci **51**: 1024–1027.

Riva CE, Sinclair SH & Grunwald JE (1981): Autoregulation of retinal circulation in response to decrease of perfusion pressure. Invest Ophthalmol Vis Sci **21**: 34–38.

Sharma RK & Netland PA (2007): Early born lineage of retinal neurons express class III beta-tubulin isotype. Brain Res **1176**: 11–17.

Stapor PC & Murfee WL (2012): Identification of class III beta-tubulin as a marker of angiogenic perivascular cells. Microvasc Res **83**: 257–262.

Sugiyama T, Moriya S, Oku H & Azuma I (1995): Association of endothelin-1 with normal tension glaucoma: clinical and fundamental studies. Surv Ophthalmol **39**(Suppl 1): S49–S56.

Ullrich N, Gillespie GY & Sontheimer H (1996): Human astrocytoma cells express a unique chloride current. NeuroReport **7**: 1020–1024.

Vinores SA, Derevjanik NL, Mahlow J, Hackett SF, Haller JA, de Juan E, Frankfurter A & Campochiaro PA (1995): Class III beta-tubulin in human retinal pigment epithelial cells in culture and in epiretinal membranes. Exp Eye Res **60**: 385–400.

Wang R (2011): Signaling pathways for the vascular effects of hydrogen sulfide. Curr Opin Nephrol Hypertens **20**: 107–112.

Received on July 30th, 2019.
Accepted on November 18th, 2019.

Correspondence:
Verena Prokosch
University Eye Hospital Mainz
Johannes Gutenberg University of Mainz
Langenbeckstrasse 1, 55131 Mainz, Germany
Tel: +49-1703862250
Fax: +49-171-0
Email: vprokosch@gmx.de

The authors thank M. Wissing and M. Landkamp-Flock for skilful technical help. The work was supported by the Deutsche Forschungsgemeinschaft (DFG) with a grant to S.T. (Th 386 20-1) and a grant to V.P. (PR 1569 1-1).